ORIGINAL ARTICLE

ANATOMICAL SOCIETY | *Journal of* Anatomy | WILEY

# Functional anatomy of the middle and inner ears of the red fox, in comparison to domestic dogs and cats

Erich Pascal Malkemper[1,2] 🆔 | Matthew J. Mason[3] 🆔 | Hynek Burda[1,2] 🆔

[1]Department of General Zoology, Faculty of Biology, University of Duisburg-Essen, Essen, Germany

[2]Department of Game Management and Wildlife Biology, Faculty of Forestry and Wood Sciences, Czech University of Life Sciences, Praha, Czech Republic

[3]Department of Physiology, Development and Neuroscience, University of Cambridge, Cambridge, UK

**Correspondence**
Erich Pascal Malkemper, Max Planck Research Group Neurobiology of Magnetoreception, Centre of Advanced European Studies and Research (caesar), Ludwig-Erhard-Allee 2, Bonn 53175, Germany.
Email: pascal.malkemper@caesar.de

**Present address**
Erich Pascal Malkemper, Max Planck Research Group Neurobiology of Magnetoreception, Center of Advanced European Studies and Research (caesar), Bonn, Germany

## Abstract

Anatomical middle and inner ear parameters are often used to predict hearing sensitivities of mammalian species. Given that ear morphology is substantially affected both by phylogeny and body size, it is interesting to consider whether the relatively small anatomical differences expected in related species of similar size have a noticeable impact on hearing. We present a detailed anatomical description of the middle and inner ears of the red fox *Vulpes vulpes*, a widespread, wild carnivore for which a behavioural audiogram is available. We compare fox ears to those of the well-studied and similarly sized domestic dog and cat, taking data for dogs and cats from the literature as well as providing new measurements of basilar membrane (BM) length and hair cell numbers and densities in these animals. Our results show that the middle ear of the red fox is very similar to that of dogs. The most obvious difference from that of the cat is the lack of a fully formed bony septum in the bulla tympanica of the fox. The cochlear structures of the fox, however, are very like those of the cat, whereas dogs have a broader BM in the basal cochlea. We further report that the mass of the middle ear ossicles and the bulla volume increase with age in foxes. Overall, the ear structures of foxes, dogs and cats are anatomically very similar, and their behavioural audiograms overlap. However, the results of several published models and correlations that use middle and inner ear measurements to predict aspects of hearing were not always found to match well with audiogram data, especially when it came to the sharper tuning in the fox audiogram. This highlights that, although there is evidently a broad correspondence between structure and function, it is not always possible to draw direct links when considering more subtle differences between related species.

**KEYWORDS**
audiogram, carnivores, cochlea, domestication, hair cells, hearing, morphology

## 1 | INTRODUCTION

Morphological differences in the auditory organs of mammals reflect adaptations to different evolutionary pressures (Fleischer, 1973; Huang et al. 2002; Mason, 2003; Mason, 2006; Rosowski et al. 2006; Mason, 2016a). This means that it is possible, at least

in principle, to predict aspects of the audition of extinct and difficult-to-test species from anatomical parameters alone (Rosowski, 1992). One approach is to search for correlations within a large collection of species, covering a broad range of body sizes and hearing abilities. Several morphological features of mammalian middle ears correlate with measurements from behavioural audiograms. Such

features include the volume of the middle ear cavity, ossicular mass, and eardrum and stapedial footplate areas (Rosowski, 1992; Hemilä et al. 1995; Coleman and Ross, 2004; Coleman and Colbert, 2010). Cochlear variables that might affect function include length and coiling, cross-sectional areas of the scalae, extent of a secondary spiral lamina, length, width and thickness of the basilar membrane (BM), and measurements of the organ of Corti including the size of the hair cells (West, 1985; Echteler et al. 1994; Vater and Kössl, 2011). However, morphological differences between the ear structures of two animals of different sizes could reflect inescapable scaling effects, rather than functionally meaningful adaptations to particular acoustic environments. One way around this problem is to compare the ears of species of comparable body size, to see whether differences in ear anatomy correspond to differences in their audiograms. This is the approach we applied in the present study.

One of the most intensively studied species in auditory biology is the domestic cat (*Felis sylvestris catus*). The use of this species as an experimental model has led to a great deal being known about the structure and function of its ear (Guinan and Peake, 1967; Spoendlin, 1969; Nedzelnitsky, 1980; Liberman, 1982; Lynch et al. 1982; Funnell et al. 1987; Peake et al. 1992; Funnell et al. 1992; Puria and Allen, 1998; Huang et al. 2000; Decraemer and Khanna, 2004). As with all experimental models, however, questions remain about how representative the cat really is of mammals as a whole, not least because this is a domestic species (Burda, 1985; Montague et al. 2014). The audition and ear anatomy of dogs have also been relatively well studied (Heffner, 1983; Braniš and Burda, 1985; Cole, 2009). Domestic dogs (*Canis lupus familiaris*) vary much more in body size than cats: larger dogs have larger tympanic membranes, but this does not appear to result in substantially different behavioural audiograms (Heffner, 1983).

Both cats and dogs are members of the order Carnivora, cats belonging to the family Felidae and dogs to the Canidae. The red fox (*Vulpes vulpes*) is a non-domesticated canid the size of a large cat or small dog. Its audiogram was recently published (Malkemper et al. 2015).

In the present study, we sought to compare middle and inner ear structures in these three carnivores. We first present a comprehensive description of the middle and inner ears of the red fox, which have previously only been mentioned as small parts of much wider studies (Doran, 1878; van Kampen, 1905; Bondy, 1907; Holz, 1931; Fleischer, 1973; Solntseva, 2010; Solntseva, 2013). Next, we present new data on dog and cat hair cell densities, filling a knowledge gap relating to these otherwise well-studied species. Finally, we highlight similarities and differences between red fox, cat and dog ears, and, by comparison with published audiograms, consider to what extent these anatomical features have recognisable functional implications.

## 2 | METHODS

### 2.1 | Morphometric analysis of the middle ears

We obtained 23 heads of wild red foxes (*V. vulpes*) from licensed hunters in the Czech Republic, based on regular shooting schedules:

no fox was killed or harmed specifically for this study. The heads of freshly shot foxes were immersion-fixed by the hunters in the field in either 10% formalin solution in water or 4% paraformaldehyde solution in 0.1 M phosphate-buffered saline (PBS). To promote tissue penetration, the hunters also injected fixative into the ear canal and the muscles surrounding the tympanic bulla. The tissues were stored in fixative for 2 weeks up to several years before dissection. One further fox was found dead in Cambridgeshire, UK, as a presumed road traffic accident. This animal was immature, as judged from the presence of both permanent and deciduous canines. Its head was removed and frozen, later to be defrosted and computed tomography (CT)-scanned (see below).

Additionally, we used 31 red fox skulls, obtained from hunters and from the collection of the Senckenberg Museum of Natural History Görlitz, for the study of middle ear ossicles. These skulls had been prepared according to standard museum procedures (Mooney et al. 1982). Briefly, the heads were boiled in water with added detergent for several hours, after which the soft tissues were manually removed from the bones. Most of the skulls were then bleached for 1–2 min in 10% hydrogen peroxide. Such procedures have no significant impact on measurements of middle ear ossicles (Nummela, 1995). The total sample comprised material from 55 red foxes (23 fixed individuals, 31 skulls and one CT-scanned head). We estimated the age of the individuals from skull measurements and defined adults as individuals with a condylobasal length (CBL) of at least 140 mm (at least 6 months of age; Hartová-Nentvichová et al. 2010; Malkemper and Peichl, 2018). For some measurements the sample size of adult animals was too small, therefore subadults were included (CBL < 140 mm). We indicate in the results whenever measurements from subadults have been included.
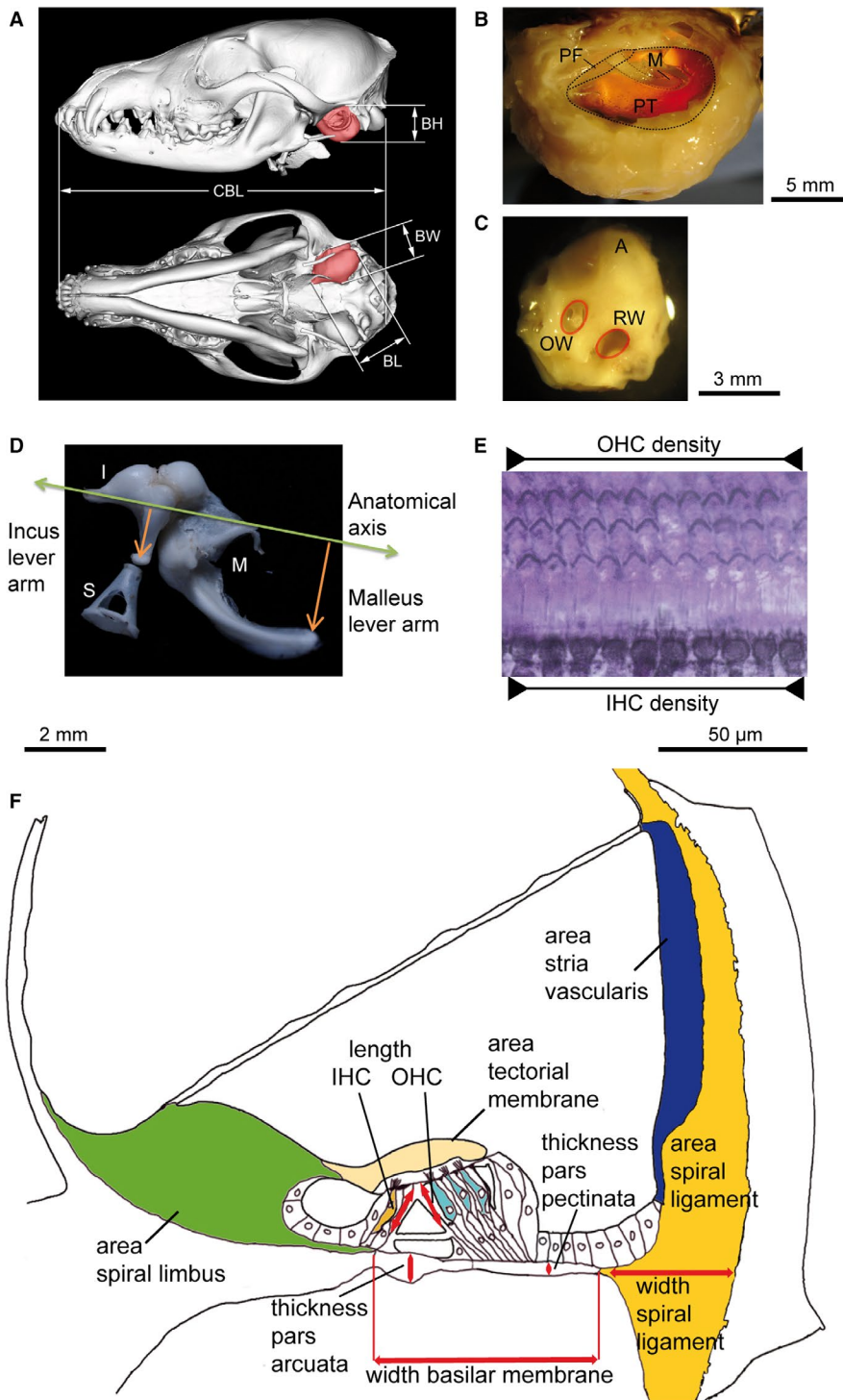
### 2.2 | Tympanic bulla

The fur, skin and masticatory muscles were removed from the skull and the lower jaws were ablated. The tympanic bullae were broken off the skull and the diameter of the proximal end of the bony external auditory meatus was determined with digital callipers. The auditory bullae were cleaned and measurements of bullar height (BH), length (BL) and width (BW) were taken with digital callipers (Figure 1A). We estimated bullar volumes from the prepared skulls as for elliptical cones, according to the formula given by Schleich and Busch (2004; Eq. 1).

$$\frac{1}{3}\left(\pi \frac{BL}{2} \times \frac{BW}{2} \times BH\right) \tag{1}$$

### 2.3 | Areas of auditory structures

The areas of the tympanic membrane pars tensa (Figure 1B) and oval window were determined by drawing the outlines on paper via

**FIGURE 1** Measurements made from the red fox middle and inner ears. (A) Computed tomography reconstruction of an immature fox skull: both permanent and deciduous canine teeth are present. The left tympanic bulla is highlighted in red and the measured anatomical variables are indicated. The condylobasal length (CBL) of this specimen was 131.3 mm. (B) Dissected bulla tympanica, with the area of the tympanic membrane indicated. (C) View onto the inner ear, with the stapes (S) footplate enclosed within the oval window (OW). The encircled areas indicate the OW and round window (RW). The position of the apex (A) where the dissection of the cochlea was started is indicated. (D) Lever arm lengths of the middle ear ossicles, measured as the perpendicular distances between the 'anatomical axis' and the tip of the ossicular processes. (E) The distance occupied by 10 inner hair cells (IHC) and three rows of 10 outer hair cells (OHC) were determined within each field of view along the whole length of the basilar membrane (1000× magnification). The distances occupied by 10 hair cells were then transformed into densities, which were presented as means of 10 segments of equal length from the apex to the base. (F) Cochlear variables determined for each half-turn of three mid-modiolar sections of each specimen (Reproduced from Davis, 1953, with the permission of the Acoustical Society of America). A, apex of promontory; BH, bulla height; BL, bulla length; BW, bulla width; I, incus; M, malleus; PF, pars flaccida of the tympanic membrane; PT, pars tensa of the tympanic membrane

a camera lucida connected to a stereomicroscope (SZH10 research stereo; Olympus, Hamburg, Germany). Each outline was drawn at two different magnifications between 7× and 70×, and digitized at 200 dpi resolution by means of a flatbed scanner. The areas (in mm$^2$) encircled by the drawn outlines were determined in ImageJ [v. 1.48v; National Institutes of Health (NIH), Bethesda, MD, USA] and, after including the magnification factor, the mean area from the two drawings was taken as the final area. All areas were thus calculated as flat surfaces from the perimeters; no account of the inflection of the tympanic membrane was made.

## 2.4 | Measurements of middle ear ossicles

Having carefully removed the auditory ossicles from the middle ear, remains of the tympanic membrane and muscle insertions were removed and the ossicles were air-dried for at least 1 week and then stored in Eppendorf tubes for later analysis. The mass of each ossicle was determined with a high-precision microbalance (MX5; Mettler-Toledo, Columbus, OH, USA). Each ossicle was weighed twice and the mean of the two measurements was taken as the final mass. High-resolution photographs were taken of each ossicle (K20D with

SMC DFA 50-mm macro objective; Pentax, Tokyo, Japan) and measurements were made from these images with IMAGEJ (1.48v; NIH).

To approximate the malleus and incus lever arms, an idealized rotational axis was defined, running from the mallear anterior process through the short process of the incus (Dahmann, 1929). This has been referred to as the 'anatomical axis' (Lavender et al. 2011; Mason, 2016a) because it does not always correspond to the true axis of rotation. The lever arms were then defined as the shortest (perpendicular) distances of the tips of the manubrium and long process of the incus to the anatomical axis (Figure 1D). Whenever available, the ossicles of both ears of an individual fox were measured, and the means were taken as the final values for that individual.

## 2.5 | Morphometric analysis of the inner ear

The cochlea was prepared using two complementary techniques: (1) surface mounts were made to estimate sensory cell numbers and density distributions and (2) mid-modiolar histological sections were made to assess dimensions at different positions along the cochlear duct.

## 2.6 | Cochlear surface mounts

To obtain surface mounts, the membranous labyrinth was carefully liberated from its bony encapsulation with fine forceps under a stereoscopic microscope. The preparation was performed in PBS. Starting in the region of the apex, each half-turn was progressively removed and instantly stained with haematoxylin for 1 min, before washing and embedding in glycerol on a microscope slide. Occasional toluidine blue staining facilitated tissue discrimination during the preparation process.

The half-turns were analysed using a brightfield microscope at 1000× magnification. The cuticular plates and stereocilia of the outer (OHC) and inner hair cells (IHC), as well as the tunnel of Corti, were readily identifiable in the toluidine blue and haematoxylin-stained cochlear surface mounts (Figure 1E). The densities of IHCs and OHCs over the course of the whole cochlear duct were determined with an eyepiece micrometer. The distance occupied by 3–10 hair cells, depending on hair cell loss, was used to calculate the number of hair cells per mm. The length of the BM was estimated by counting the number of non-overlapping fields of view along the tunnel of Corti. All determined parameters were assigned to 10% segments relative to the length of the BM of the respective individual in order to standardize them for inter-individual comparisons. We prepared surface specimens of 10 cochleae (seven left ears, three right ears) from eight different foxes (including subadults) to count the hair cells. In two animals, both ears were analysed and we used the mean of both cochleae for each position on the BM.

In addition to the red fox specimens, cochlear surface mounts of three domestic cats, 4 months of age, and four adult domestic dogs (beagles) were prepared in a similar way, to determine hair cell numbers and density gradients. The cat and dog ears were formalin immersion-fixed specimens obtained from the Institute of Experimental Medicine of the Czech Academy of Sciences. The data had been collected in 1979 by author H.B., but have not been published previously.

## 2.7 | Cochlear sections

To obtain cross-sectional data from cochlear structures, the inner ear was decalcified in 25% EDTA in PBS (pH = 8.0) for 3–4 weeks at 4°C. The EDTA solution was exchanged at least once per week. After decalcification, the cochleae were embedded in paraffin-celloidin (Ballast, 1984; Burda et al. 1988). Briefly, the decalcified and ethanol-dehydrated cochleae were incubated in a 1:1 mixture of diethyl ether and 100% ethanol for 4 h. They were then incubated for 3 days in 2–4% Collodion (Fluka Chemie, Buchs, Switzerland) solution, followed by 4 days' incubation in 4–8% Collodion solution. Care was taken to remove all air bubbles trapped in the specimens during these incubation steps. Afterwards, the cochleae were hardened in chloroform overnight, cleared for 4 h in xylene, and embedded in paraffin. Microtome sections (15 μm) were taken until the plane of the modiolus was passed, which was assessed by regular microscopic examination. The sections were stretched in a water bath containing 10% ethanol at 40°C and mounted on positively charged slides (Superfrost Plus®; Menzel, Braunschweig, Germany). Sections were dried on a heat plate (61°C) and stained with haematoxylin and eosin. They were mounted with Roti Histokit I® and examined by light microscopy (BX40; Olympus). Digital images of the sections were taken with a CCD camera (XC30; Olympus) and the image-processing software analysis (V. 5.0; Olympus soft imaging solutions, Münster, Germany). Measurements were made in IMAGEJ.

The ears of eight red fox individuals (subadult and adult) were sectioned. From two of these animals, both ears were processed and the results averaged. Three mid-modiolar sections were chosen from each specimen and the following variables determined for each half-turn (Figure 1F): length (size, height) of the IHC and one OHC, width of the BM, maximal thickness of the BM homogeneous ground substance (zona arcuata, z. pectinata), cross-sectional area of the stria vascularis, area and maximal thickness of the spiral ligament (without stria vascularis), area of the tectorial membrane, presence (in % of spiral ligament width) of an osseous spiral lamina, area of the limbus spiralis.

## 2.8 | CT scanning

One immature fox head (CBL = 131.3 mm) was available for CT scanning. After defrosting, the head was skinned, trimmed and wrapped in cellophane before mounting in a Nikon XT H 225 CT scanner at the Cambridge Biotomography Centre. Two 1000-ms exposure images were averaged at each of 1080 projection angles, using settings of 140 kV and 95 μA. Cubic voxel side-lengths were 74 μm. Following the whole-head scan, the right auditory bulla was dissected out using an electric circular saw. This specimen was trimmed, wrapped in cellophane and scanned as above to obtain images at 20-μm voxel side-length.

Reconstruction software included CT Agent XT 3.1.9 and CT Pro 3D XT 3.1.9 (Nikon Metrology, 2004–2013). The tomograms were converted to 8-bit jpg files in Adobe Photoshop CS 8.0 (Adobe Systems Inc., 2003). 3D reconstructions of the skull were then made from these files using MicroView 2.5.0 (Parallax Innovations Inc., 2017). Reconstructions of the ear structures were made using Stradwin 5.4 (Graham Treece, Andrew Gee & Richard Prager, 2018, https://mi.eng.cam.ac.uk/Main/StradWin), in a procedure requiring manual segmentation of structures' boundaries from the tomograms. Middle ear cavity volume was calculated from these reconstructions (ossicle and muscle volumes were not included in this measurement). To make cochlear measurements, we reoriented the tomograms in MicroView, such that the z-axis ran through the centre of the modiolus. Then we recorded the 3D coordinates of multiple points along the centre of the cochlear canal, starting from the beginning of the primary spiral lamina near the round window and extending to the apex. At least one point was recorded every 10° along the spiral. The total length of the cochlear canal was estimated as the sum of the linear distances between consecutive points. The number of spiral turns and the radii of curvature at different points were established from the x-y coordinates of these points (Mason et al. 2016).

## 2.9 | Statistics

Sigmaplot (V. 12.5, Systat Software Inc.) and GraphPad Prism (V. 8; GraphPad Software) were used to plot the graphs and calculate statistics. Variance equality and normal distribution were tested with Bartlett's test and the Shapiro–Wilk test, respectively. For normal distributions and equal variances, t-tests or analysis of variance (ANOVA) were used, depending on the structure of the data. Pearson product moment correlation was used to test for correlations. To reduce the chance of type I error given the multiple analyses, we performed Bonferroni correction, which reduced the α-level of significance from 0.05 to 0.004. Graphical metrics and cell counts were made using ImageJ (1.48v; NIH).

## 3 | RESULTS

### 3.1 | Middle ear morphology of the red fox

#### 3.1.1 | Tympanic bulla and tympanic membrane

The tympanic bulla in the adult red fox protruded distinctly from the skull base (Figure 1A) and was of ovoid shape [mean ± SD length 20.2 ± 0.9 mm, height 16.7 ± 0.5 mm, width 11.8 ± 1.2 mm; n = 11 foxes]. The mean ± SD adult bullar volume, estimated as an ovoid from the skulls, was 1048 ± 168 mm$^3$ (n = 11 foxes). This is strikingly close to the bullar volume of 1095 mm$^3$, measured more accurately from CT reconstructions in one immature animal (Figure 2). The great majority of the middle ear cavity volume was contained within the auditory bulla. The shape of this cavity was relatively simple, although a low ridge extended in a rostroventral direction from just ventral to the round window to below the cochlear promontory, while a second ridge extended from just below where the first ended to the anteroventral wall of the cavity. Together, these ridges served to demarcate the voluminous caudoventral part of the cavity from the rostrodorsal component, which contained the promontory and ossicles. The cochlear promontory was a low bulge, not at all prominent, caudal to which was
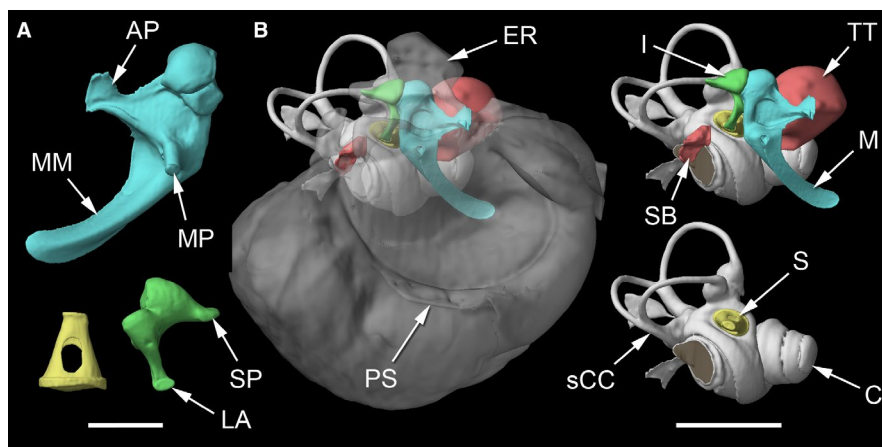


**FIGURE 2** The red fox middle ear. (A) Computed tomography (CT) reconstructions of the right middle ear ossicles of the red fox. The malleus (blue) and incus (green) are shown from approximately medial views, while the stapes (yellow) is shown from a dorsal view. Scale bar 2 mm. (B) Micro-CT reconstructions of the right middle and inner ear structures of the red fox, in approximately lateral views. The main reconstruction shows all modelled structures: the internal boundaries of the middle ear cavity (including tympanic membrane) are shown in translucent grey. The malleus is shown in blue, the incus in green and the two middle ear muscles in pink. In the top right image, the middle ear cavity has been removed and the round window has been shaded in brown. In the bottom right image, the malleus, incus and the two middle ear muscles have also been removed to reveal more of the bony labyrinth (white). The canals for the endolymphatic and perilymphatic ducts are included in the reconstruction. AP, anterior process of malleus; C, cochlea; ER, epitympanic recess; I, incus; LA, lenticular apophysis of incus; M, malleus; MM, manubrium of malleus; MP, muscular process of malleus; PS, partial septum within middle ear cavity; S, stapes; SB, stapedius muscle belly; sCC, secondary crus commune; SP, short process of incus; TT, tensor tympani muscle belly

a recess for the round window. A small epitympanic recess extended a short distance dorsal to the heads of the malleus and incus, and a posterior extension from this recess accommodated the short process of the incus. The tympanic membrane (pars tensa) was of oval shape and had a mean area of 55.7 ± 7.9 mm$^2$ ($n$ = 16 foxes, including subadults). The small pars flaccida of the tympanic membrane, situated dorsally, amounted to < 10% of the total tympanic membrane area (Figure 1B).

### 3.1.2 | Middle ear ossicles

The CT reconstructions of the middle ear ossicles are shown in Figure 2A. The malleus did not possess an orbicular apophysis. Its small transversal lamina expanded distally into a short anterior process, which was indistinguishably synostosed with the wall of the middle ear cavity. The manubrium of the malleus was very robust, with a wide inserting margin and prominent lateral process, and it curved rostrally. Overall, it made an angle of ~45° with the anatomical axis of ossicular rotation (Figure 1D). At the base of the manubrium was an unusually long and sturdy muscular process for the insertion of the musculus tensor tympani. This muscle had a very large, almost spherical body located within a deep, bony recess just rostral to the oval window (Figure 2B). The complex, multifaceted articulation between malleus and incus was not fused. Like the malleus, the incus was solidly built. Its processes appeared quite narrow from a lateral view, but wider from a posterior view. The short process had a ligamentous articulation with the skull within the posterior extension of the epitympanic recess, while the long process terminated in an oval lenticular apophysis for articulation with the stapes. Our impression during dissection was that the malleus and incus were stiffly articulated with each other, and the malleus was also stiffly articulated with the wall of the tympanic cavity.

The stapes had the shape of a flattened cone. The crura were hollow, as was the neck region of the ossicle where the crura unite. The footplate, convex on its vestibular side, was made of very thin bone with a thickened labrum. It fitted tightly within the oval window. The intercrural foramen was relatively small; no stapedial artery passed through it. There was a very small muscular process for the insertion of the stapedius tendon near the head of the stapes, posteroventrally. The stapedius muscle belly was found within a bony recess and was considerably smaller in volume than the tensor tympani (Figure 2B).

The adult malleus mass was 11.42 ± 0.93 mg ($n$ = 8 foxes). Adult incus mass was 5.44 ± 0.63 mg ($n$ = 11 foxes) and adult stapes mass 0.66 ± 0.12 mg ($n$ = 7 foxes). The lever arm length of the adult red fox malleus was 3.60 ± 0.60 mm ($n$ = 5 foxes). The lever arm length of the incus was 1.62 ± 0.18 mm ($n$ = 11 foxes). The resulting mean malleus-to-incus lever arm ratio was 2.22. The stapes footplate, as determined from the size of the oval window (Figure 1C), had a mean area of 1.82 ± 0.2 mm$^2$ ($n$ = 7 foxes). The resulting mean area ratio between the tympanic membrane (pars tensa only) and the oval window was 30.6. Finally, we calculated the impedance transform ratio (ITR), defined as the lever ratio multiplied by the area ratio (Mason, 2016b). The average red fox ITR was 67.3.

### 3.1.3 | Postnatal development of the red fox middle ear

To elucidate the effect of postnatal development on middle ear dimensions in the red fox, we studied specimens from several-week-old pups to several-year-old adults, and tested for correlations between ear measurements and an age-related morphometric variable of the skull, the CBL (Hartová-Nentvichová et al. 2010).

The proximal diameter of the bony auditory meatus increased with increasing CBL (minimum 3.8 mm, maximum 6.75 mm, mean 5.85 ± 0.68 mm; $R^2$ = 0.61, $P$ < 0.001, $n$ = 26 foxes). The area of the tympanic membrane pars tensa was not significantly correlated with CBL after Bonferroni correction ($R^2$ = 0.39, $P$ = 0.009, $n$ = 16 foxes). The area of the pars flaccida was not analysed. The volume of the bulla tympanica increased with increasing CBL (Table S1; $R^2$ = 0.24, $P$ < 0.001, $n$ = 38 foxes). Bullar volumes doubled during early postnatal development, ranging from 678 mm$^3$ to 1412 mm$^3$.

The masses of the malleus and incus were positively correlated with age (Figure S1, Table S1; malleus, $R^2$ = 0.54, $P$ < 0.001, $n$ = 41 foxes; incus, $R^2$ = 0.41, $P$ < 0.001, $n$ = 47 foxes). For the stapes the same trends were apparent, but the correlation was not significant after Bonferroni correction ($R^2$ = 0.18, $P$ = 0.034, $n$ = 25 foxes). Of the measured linear ossicle dimensions, only the incus lever arm significantly increased with age ($R^2$ = 0.19, $P$ < 0.003, $n$ = 47 foxes). Individual ITRs varied between 53.4 and 99.9, but showed no correlation with age ($R^2$ = 0.00, $P$ = 0.982, $n$ = 13 foxes).

## 3.2 | Inner ear

### 3.2.1 | Vestibular system

The vestibular apparatus of the red fox was not examined in detail. Its general structure, as seen from the CT reconstruction, was similar to that of the dog (Ekdale, 2013). A secondary crus commune was formed by the fusion of the bony tubes for the lateral and posterior semicircular canals (Figure 2B), although the contributions of the two tubes could still be discerned from its figure-of-eight cross-section. Bony passages for both endolymphatic and perilymphatic ducts were observed and are included in the reconstructions of Figure 2B.

### 3.2.2 | Cochlear dimensions

The red fox cochlea had 3.4 turns ($n$ = 1, CT-scanned specimen). An elongated part in the basal region (cochlear hook) was well developed and the basal turn of the cochlea was significantly wider than the apical turns. The length of the BM, as determined from surface specimens, was 25.8 ± 1.6 mm ($n$ = 8 foxes including subadults), while the CT reconstruction yielded a cochlear duct length of 25.7 mm ($n$ = 1). The BM length did not correlate with CBL ($R^2$ = 0.14, $P$ = 0.367, $n$ = 8 foxes). The cat BM length was 27.4 ± 0.3 mm ($n$ = 3 cats); the value for the dog (beagle) was

27.6 ± 0.3 mm (*n* = 4 dogs). The red fox BM was not significantly different in length from that of the dog (two-tailed *t*-test: *t* = 2.21, *P* = 0.052) or the cat (*t* = 1.69, *P* = 0.126).

The organ of Corti of the red fox exhibited all the typical mammalian structures and cell types. As in other mammals, the different components of the red fox's cochlear partition changed in size and shape along the cochlear duct, as described below (Figure 3). The mean values of the different variables at different half-turns assessed from mid-modiolar cochlear sections are shown in Table 1.

The BM in our red fox specimens reached a maximal thickness of 17.7 ± 2.8 μm (average of pars pectinata and pars arcuata) in the region of the first half-turn (*n* = 8 foxes). Further basally in the hook region, the thickness slightly decreased by ~1–2 μm (Table 1). From the first half-turn towards the apex, the thickness of the BM decreased constantly until it reached a minimal value of 5.8 ± 2.6 μm (*n* = 3 foxes) in apical regions. The decrease in BM thickness towards the apical end was accompanied by an increase in BM width, which was narrowest in the basal hook region (83 ± 34 μm, *n* = 6 foxes) and reached maximal width (384 ± 10 μm, *n* = 3 foxes) near the apex. The stiffness ratio f (thickness BM/width BM; von Békésy, 1960) decreased from a basal value of ~0.19 to an apical value of 0.015 (f basal: f apical = 13:1). The cross-sectional area of the stria vascularis increased from the apex (2876 ± 652 μm², *n* = 3 foxes) towards the base (12 880 ± 1940 μm², *n* = 5 foxes).

### 3.2.3 | Hair cell variables

The general arrangement of the hair cells in the red fox cochlea followed the typical mammalian *bauplan*, with three rows of OHCs and a single row of IHCs running along the tunnel of Corti. Infrequently, a fourth row of OHCs was observed, predominantly in the more apical regions (Figure S2). The lengths of the IHCs did not change much along the cochlear duct (range of the half-turn means: 21.7–27.9 μm; Table 1), while the lengths of the OHCs increased from 21.2 ± 1.8 μm (*n* = 3 foxes) in the hook region to 37.7 ± 1.2 μm (*n* = 4 foxes) in the apical region (Table 1).

Densities of IHCs in the red fox changed only moderately along the length of the cochlear duct (Figure 4), and the IHC density differences at different positions of the BM were not significant (two-way ANOVA: *F* = 1.580, *P* = 0.142, *n* = 8 foxes). The overall mean IHC density in the red fox was 107 ± 3 IHCs/mm (*n* = 8). There was a trend towards a local IHC maximum (113 ± 12 IHCs/mm, *n* = 8) close to the base, 71–80% of the distance along the BM from the apex. OHC densities in the red fox were almost constant along the cochlear duct, with a mean of 408 ± 9 OHCs/mm (*n* = 8; Figure 4). The extrapolated total hair cell numbers for the red fox cochlea were 2757 ± 218 IHCs (*n* = 8) and 10 502 ± 860 OHCs (*n* = 8).

### 3.2.4 | Hair cell densities in the dog (beagle)

Densities of IHCs in the dog were intermediate between those of the cat (see below) and red fox and changed only moderately along the course of the cochlear duct (Figure 4). The overall mean IHC density was 101 ± 3 IHCs/mm (*n* = 4 dogs). As in the fox and cat (see below), a trend towards a local maximum was found near the base, having 108 ± 6 IHCs/mm (*n* = 4) in the dog. OHC densities in the dog were
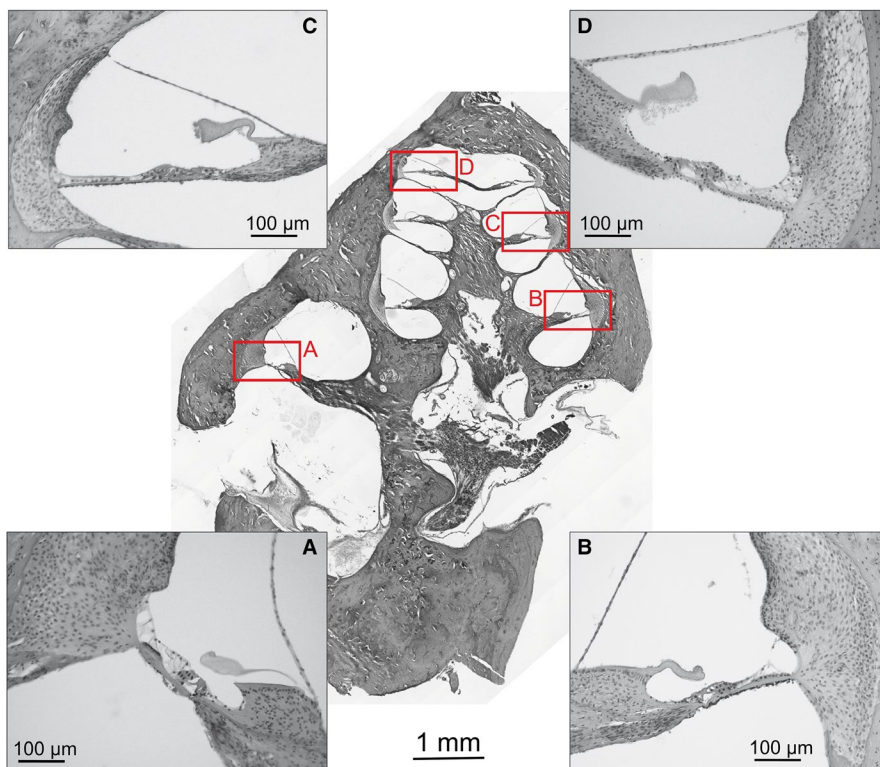


**FIGURE 3** Mid-modiolar haematoxylin and eosin stained section of the cochlea of the red fox with representative sections at different positions along the cochlear duct. Inset (A) depicts the typical situation in the region of the most basal half-turn with a thick and narrow basilar membrane, while inset (D) shows the situation in the most apical half-turn with a wide and thin BM. Other insets (B, C) correspondingly show intermediate HTs. For a description of the quantitative changes of the cochlear partition, see the main text and Table 1

**TABLE 1** Cochlear variables assessed from mid-modiolar sections of red fox cochleae

| | | Hook | HT1 | HT2 | HT3 | HT4 | HT5 | HT6 | HT7 |
|---|---|---|---|---|---|---|---|---|---|
| | | DfB <1 mm | DfB 1 mm | DfB 6.8 mm | DfB 11.3 mm | DfB 15.4 mm | DfB 18.9 mm | DfB 22.1 mm | DfB 25 mm |
| Thickness BM pars arcuata, μm | Mean | 16.2 | 17.7 | 16.8 | 14.4 | 11.9 | 9.5 | 7.0 | 5.8 |
| | SD | 2.1 | 2.8 | 3.1 | 2.6 | 2.4 | 2.4 | 1.7 | 2.6 |
| | n | 6 | 8 | 8 | 8 | 8 | 8 | 8 | 3 |
| Thickness BM pars pectinata, μm | Mean | 15.9 | 17.7 | 14.9 | 11.8 | 10.0 | 8.0 | 6.5 | 5.4 |
| | SD | 1.3 | 2.2 | 2.3 | 2.3 | 2.0 | 1.1 | 1.6 | 1.8 |
| | n | 6 | 8 | 8 | 8 | 8 | 8 | 8 | 3 |
| Width BM, μm | Mean | 83 | 188 | 259 | 268 | 282 | 322 | 371 | 384 |
| | SD | 34 | 26 | 33 | 23 | 17 | 33 | 40 | 10 |
| | n | 6 | 8 | 8 | 8 | 8 | 8 | 8 | 3 |
| Width spiral ligament (radial), μm | Mean | 424 | 334 | 212 | 154 | 125 | 122 | 94 | 82 |
| | SD | 37 | 60 | 35 | 13 | 9 | 15 | 21 | 9 |
| | n | 5 | 8 | 8 | 8 | 8 | 8 | 8 | 3 |
| Cross sectional area stria vascularis, μm$^2$ | Mean | 12 880 | 10 324 | 11 376 | 9364 | 6666 | 6131 | 6839 | 2876 |
| | SD | 1949 | 2720 | 3155 | 1885 | 1569 | 2892 | 4708 | 652 |
| | n | 5 | 8 | 8 | 8 | 8 | 8 | 8 | 3 |
| Osseous support of spiral ligament, % | Mean | 94 | 75 | 38 | 25 | 13 | 0 | 0 | 0 |
| | SD | 5 | 14 | 16 | 7 | 13 | 0 | 0 | 0 |
| | n | 5 | 8 | 8 | 8 | 8 | 8 | 8 | 3 |
| Cross sectional area spiral ligament, μm$^2$ | Mean | 163 471 | 151 614 | 129 212 | 102 857 | 66 051 | 51 665 | 31 964 | 20 023 |
| | SD | 25 183 | 24 918 | 18 906 | 22 058 | 9557 | 10 129 | 7786 | 4311 |
| | n | 5 | 8 | 8 | 8 | 8 | 8 | 8 | 3 |
| Cross sectional area tectorial membrane, μm$^2$ | Mean | 835 | 2369 | 4482 | 5109 | 5214 | 7029 | 7870 | 6457 |
| | SD | 316 | 1148 | 1744 | 1979 | 1574 | 2920 | 3648 | 2162 |
| | n | 5 | 8 | 8 | 8 | 8 | 8 | 8 | 3 |
| Length IHC, μm | Mean | 21.7 | 25.4 | 24.7 | 25.5 | 24.6 | 24.3 | 27.9 | 26.8 |
| | SD | | 3.8 | 2.3 | 7.2 | 4.9 | 3.5 | 4.6 | 6.0 |

(Continues)

**TABLE 1** (Continued)

| | | Hook | HT1 | HT2 | HT3 | HT4 | HT5 | HT6 | HT7 |
|---|---|---|---|---|---|---|---|---|---|
| | n | 1 | 4 | 3 | 2 | 4 | 4 | 5 | 2 |
| Length OHC, μm | Mean | 21.2 | 24.1 | 26.3 | 29.2 | 32.3 | 36.2 | 37.7 | 49.3 |
| | SD | 1.8 | 2.4 | 2.9 | 3.3 | 4.4 | 4.4 | 1.2 | |
| | n | 3 | 7 | 7 | 7 | 7 | 5 | 4 | 1 |
| Cross sectional area limbus spiralis, μm² | Mean | 21 649 | 22 615 | 22 512 | 19 602 | 14 438 | 13 051 | 9346 | 6511 |
| | SD | 3268 | 3931 | 3820 | 3619 | 2965 | 2072 | 2150 | 1492 |
| | N | 5 | 8 | 8 | 8 | 8 | 8 | 8 | 3 |

BM, basilar membrane; DfB, distance from the base; HT, half-turn; IHC, inner hair cells; n, number of individuals; OHC, outer hair cells.
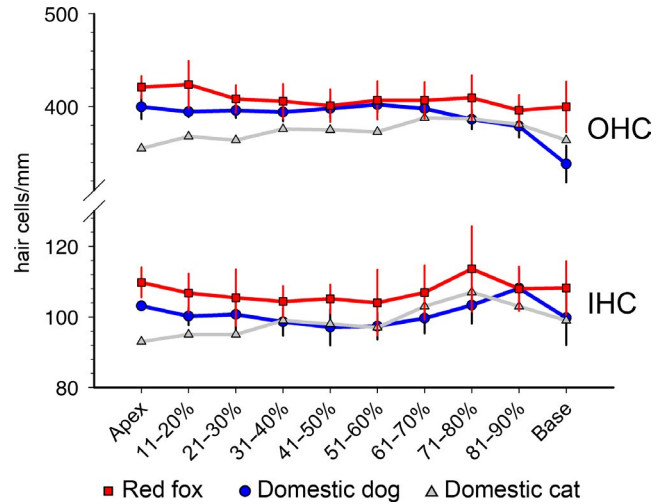


**FIGURE 4** Inner (IHC) and outer hair cell (OHC) densities along the cochlear duct in the red fox, dog, and cat (means ± SD). All species showed highest IHC densities near the base where the frequency of best hearing is represented. Red fox ($n = 8$); domestic dog (beagle, $n = 4$), domestic cat ($n = 3$, SD unknown)

almost constant along the cochlear duct, with a mean of 389 ± 19 OHCs/mm ($n = 4$; Figure 4). The extrapolated total hair cell numbers for the dog cochlea were 2775 ± 123 IHCs ($n = 4$) and 10 702 ± 245 OHCs ($n = 4$).

### 3.2.5 | Hair cell densities in the cat

Densities of IHCs in the cat were lower than in the red fox, and changed only moderately along the course of the cochlear duct (Figure 4). The overall mean IHC density was 99 IHCs/mm ($n = 3$ cats, no SD is available for this species). From the apex with a mean density of 93 IHCs/mm ($n = 3$), the number increased steadily to a local maximum of 107 IHCs/mm ($n = 3$) at 71–80% of the distance along the BM from the apex, after which density slightly decreased to 99 IHCs/mm ($n = 3$) at the basal end. Similarly to the red fox, OHC densities in the cat were almost constant along the cochlear duct, but the mean of 373 OHCs/mm ($n = 3$) was lower (Figure 4). The average extrapolated total hair cell numbers for the cat cochlea were 2723 IHCs ($n = 3$) and 10 105 OHCs ($n = 3$).

## 4 | DISCUSSION

The shapes of the audiograms of cats, dogs and foxes are similar, with the fox audiogram generally taking an intermediate position between those of dogs and cats (Figure 5). One of the more obvious differences is that the cat has an extended high-frequency range compared to the two canids (hearing limits at 60 dB sound pressure level cat: 79 kHz, red fox: 48 kHz, dog: 44 kHz). Another is that the fox audiogram is more sharply tuned around its best sensitivity at 4 kHz. However, given the low numbers of animals
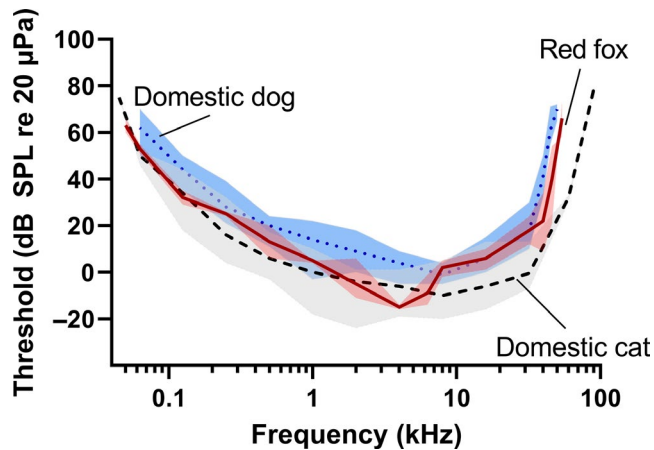
**FIGURE 5** Behavioural audiograms of the red fox, cats and dogs. Note the striking similarities between the audiograms over a wide range of frequencies, although cats have a higher upper frequency limit, while hearing of foxes appears to be more sharply tuned. Shaded areas indicate the range of thresholds between individuals of the same species. Domestic cat (84 cats, taken from 10 different audiograms collected by Fay, 1988); domestic dogs (four dogs of different breeds; Heffner, 1983); red fox (three foxes; Malkemper et al., 2015)

sampled and the different experimental laboratories in which the tests were performed, we cannot be sure that these audiogram features reflect genuine species differences. We were interested to see what the auditory anatomy leads us to predict about the relative hearing abilities of these animals.

## 4.1 | Middle ear

The middle ear apparatus of the fox is, as expected, very similar to that of dogs and other canids, as described elsewhere (Keen and Grobbelaar, 1941; Hunt, 1974; Mason, 1999; Cole, 2009; Evans and De Lahunta, 2013). Table 2 compares measured middle ear variables among carnivores. The very robust, curved manubrium of the malleus, with wide inserting margin, appears to be characteristic of canids; that of the cat is relatively thin and straight. While the cat has a well-developed septum within its bullar cavity, which divides it into two subcavities, connected through a narrow foramen within the septum (Hunt, 1974; Peake et al. 1992; Huang et al. 2002), the middle ear cavity of the fox (and dogs) has only a trace of such a division, as represented by the low ridges extending across the medial wall.

### 4.1.1 | Ideal transformer models

The function of the middle ear is to increase the proportion of incident sound energy that is transmitted from the ear canal to the fluid-filled cochlea. The ITR is often used to compare hearing sensitivity among species, according to a model of the middle ear as an 'ideal transformer'. It is calculated in the present study

as the product of the area ratio between the tympanic membrane and the oval window, and the lever ratio resulting from the rotation of the ossicles around an anatomically defined axis (Dallos, 1973; Webster and Webster, 1975; Hunt and Korth, 1980; Mason, 2004; Begall and Burda, 2006; Coleman and Colbert, 2010). The average ITRs are 63 in the cat, 52 in the dog and 67 in the red fox (Table 2), but there were large intra-specific differences among our red fox individuals, and their ITRs actually varied between 53.4 and 99.9. ITRs have been used to calculate transmission efficiencies for a wide range of mammalian species (Dallos, 1973; Webster and Webster, 1975; Hunt and Korth, 1980); however, these calculations are heavily dependent on the value of the specific acoustic impedance of the cochlea that is chosen. In these other studies this was 56 kPa s m$^{-1}$ for all species, based originally on a value determined for humans (Zwislocki, 1965). The true specific acoustic impedances of red fox cochleae are unknown, but unless they vary substantially among individuals, to match the range in ITR values, we would predict a wide range of transmission efficiencies. Quite apart from this issue, ideal transformer models ignore energy losses attributable to friction and also ignore elasticity and inertia, which lead to frequency-dependent middle ear impedances. For such reasons, the functional relevance of anatomically calculated ITRs has been strongly challenged (Rosowski and Graybeal, 1991; Rosowski et al. 2006; Mason, 2016b). It is difficult to believe that they could be used accurately to predict differences in hearing sensitivity in closely related species.

### 4.1.2 | Middle ear compliance

To overcome one of the major shortcomings of ideal transformer models, one would have to factor in compliances and inertias (reactances), which contribute to the overall middle ear impedance. The volume of the middle ear cavity is one of the factors affecting middle ear compliance, which in turn affects low-frequency hearing (Ravicz et al. 1992). The total middle ear cavity volume of the red fox (adult mean 1048 mm$^3$) is very similar to that of the cat (domestic cat: 900 mm$^3$, European wildcat: 1070 mm$^3$; Huang et al. 2002). Kirikae (1960) reported middle ear cavity volumes between 440 and 1740 mm$^3$ for six dogs with body masses between 5 and 18 kg (mean 1150 mm$^3$), while Defalque et al. (2005) calculated volumes between ~200 and 2750 mm$^3$ for 18 mesaticephalic dogs between ~2 and 55 kg (mean 1500 mm$^3$). The four dog breeds tested by Heffner (1983) ranged in size from Chihuahua to Saint Bernard, and so presumably had very different cavity volumes, and yet there is little difference in their low-frequency audiograms (Figure 5). This is consistent with the notion that ossicular stiffness rather than middle ear volume limits middle ear compliance in larger mammals like dogs (see below). However, the doubling of bullar volume during early adulthood in the red fox allows for the possibility of an ontogenetic improvement in low-frequency sensitivity.

The middle ear cavity of cats is characterised by a perforated septum, which divides it into two acoustic chambers (Keen and Grobbelaar, 1941).

**TABLE 2** Middle and inner ear parameters of several carnivore species. Data from the present work are indicated in bold.

| Common name | Scientific name | Middle ear | | | | | | Inner ear | | | | | |
|---|---|---|---|---|---|---|---|---|---|---|---|---|---|
| | | Bullar volume, mm³ | Tympanic membrane area, mm² | Oval window area, mm² | Mean area ratio | Ossicular lever ratio | ITR | Cochlear turns | BM length, mm | BM width basal-apical, mm | BM thickness basal-apical, μm | Total IHC | Total OHC |
| Red fox | *Vulpes vulpes* | **1048** | **55.7** | **1.8** | **30.6** | **2.2** | **67** | **3.2** | **25.78** | **0.08–0.45** | **17.7–5.5** | **2757** | **10 502** |
| Domestic dog | *Canis familiaris* | 200–2750[28,27] | 30–63.3[4,24] | 1.96–2.0[24,25] | 23.6 | 1.6[25] | 52 | 3–3.5[10,11,13,18] | 22.1–28[1,2,7,8,9,11]; **27.6** | 0.24–0.4[2,10] 0.29[30] (basal) | | 2603[2] **2775** | 10 548[2] **10702** |
| Domestic cat | *Felis catus* | 900[26] | 41[15] | 1.12–1.3[15,29,21] | 33.9 | 2[15] | 63 | 3[13,10]; >3[18] | 20–28[3,5,6,8,9,12,12,19,20,22,23]; **27.4** | 0.08–0.43[3,10,17,22] | 13.5–5[3]; 12–5[19] | **2723** | **10105** |
| Jaguar | *Panthera onca* | | 58[16] | 2.1[16] | 27.6 | 2.8[16] | 77 | 2.75[16] | 33.3[16] | | | 3354[14] | 13 076[14] |
| Tiger | *Panthera leo* | 13 200[16] | 61[16] | 3.5[16] | 17.4 | 2.8[16] | 49 | 2.75[16] | 35.5[16] | | | 3414[14] | 12 936[14] |

BM, basilar membrane; IHC, inner hair cells; ITR, impedance transform ratio; OHC, outer hair cells.

[1]Mair (1976).
[2]Braniš and Burda (1985).
[3]Cabezudo (1978).
[4]Heffner (1983).
[5]Sato et al. (1999).
[6]Liberman (1982).
[7]Igarashi et al. (1972).
[8]Schuknecht et al. (1965).
[9]Keen (1940).
[10]Keen (1939).
[11]Le and Keithley (2007).
[12]West and Harrison (1973).
[13]West (1985).
[14]Ulehlova et al. (1984).
[15]Puria and Allen (1998).
[16]Burda et al. (1984).
[17]Echteler et al. (1994).
[18]Gray (1907).
[19]Ketten (1997).
[20]Liberman and Beil (1979).
[21]Salih et al. (2012).
[22]Retzius (1884).
[23]Schuknecht (1953).
[24]Hemilä et al. (1995).
[25]Mason (1999).
[26]Huang et al. (2002).
[27]Defalque et al. (2005).
[28]Kirikae (1960).
[29]Lynch et al. (1982).
[30]Fleischer (1973).

The septum is believed to produce a frequency-dependent change in functional cavity volume (Peake et al. 1992). At low frequencies, the two subcavities are acoustically coupled through the hole in the septum, so that the whole bullar volume contributes to the middle ear cavity compliance. At higher frequencies, the acoustic mass represented by the hole in the septum will act to decouple the two cavities, with resonance expected somewhere in-between. The septum thereby introduces an impedance peak at ~4 kHz at which frequency sound transmission is expected to be reduced, but it simultaneously eliminates a sharp peak at 10 kHz which might otherwise interfere with sound source localisation (Huang et al. 2000). This divided middle ear cavity structure is found in felids (Huang et al. 2000) but not in canids (Hunt, 1974). There is no septum in the red fox bulla, although there are ridges in the middle ear cavity wall below the cochlear promontory which probably represent the 'pseudosepta' referred to by Hunt (1974). Whether canids experience higher-frequency impedance peaks is unknown, but it is not apparent from their behavioural audiograms. In fact, the frequency of best hearing in red foxes is at 4 kHz (Figure 5), coinciding with the impedance peak in cat middle ears.

While middle ear cavity compliance tends to dominate impedance at low frequencies in small mammals such as rodents, tympanic-ossicular stiffness becomes more important in larger mammals (Ravicz et al. 1992). The stiffness of the articulation between the anterior process of the malleus and the skull can range from a very firm anchorage in ancestral and 'microtype' middle ears to a much looser connection in 'freely mobile' (Fleischer, 1978) and 'Ctenohystrica-type' (Mason, 2013) middle ears. Cats, dogs and foxes are best categorised as having 'transitional-type' ossicles (Fleischer, 1978), featuring relatively large malleus and incus heads, no orbicular apophyses and manubria at an angle somewhere between 0 and 90 degrees to the anatomical axis. Fleischer (1978) described transitional mallei as having an anterior process (gonial) which is normally fused to the tympanic bone. A comparative study confirmed a synostosis in extant carnivores of 12 different families, including the cat and dog (Wible and Spaulding, 2012); our CT data revealed the same feature in the red fox (Figure 2). Although the anterior process appears stiffly attached to the skull in dissections, the connection is quite narrow and may be much more flexible *in vivo*, when the structures are hydrated.

In conclusion, based on bullar volume and from what we could tell of ossicular stiffness, there is no reason to believe that overall middle ear stiffness in the fox differs significantly from that of the dog and cat. This is consistent with the fact that all these species have similar low-frequency hearing sensitivities (Figure 5).

### 4.1.3 | Ossicle mass

'Lumped element' models of middle ear function typically work on the principle that ossicular mass has the dominant effect on middle ear impedance at high frequencies (Hemilä et al. 1995). Accordingly, one would expect a significantly lower ossicular mass in the cat, which has better high frequency hearing compared to the fox and dog; however, our data do not support this: cat ossicular masses are only slightly lower than those of the red fox (red fox: malleus: 11.4 mg, incus: 5.4 mg, stapes: 0.7 mg; cat: malleus: 10.2 mg, incus: 4.4 mg, stapes: 0.56 mg; Nummela, 1995). Furthermore, the ossicular masses in a dog of unspecified breed were found to be considerably larger than in the fox (malleus: 18.64 mg, incus: 9.3 mg, stapes: 0.99 mg; Nummela, 1995). Mason (1999) reported even heavier ossicles from one greyhound (malleus: 24.4 mg, incus: 11.46 mg). Ossicular mass therefore varies by at least 25% between individual dogs, and likely considerably more if the smallest and largest breeds are considered. The fact that Heffner (1983) found no clear difference between the high frequency hearing limits of a Chihuahua and a Saint Bernard (Figure 5) further indicates that ossicle mass is unlikely to limit high frequency hearing in these animals. 'Lumped element' electrical analogue models become increasingly unreliable at higher frequencies, at which the wavelengths of sound approach the dimensions of the auditory structures (Fletcher, 1992). Indeed, experimental evidence from some species suggests that the middle ear may not limit high-frequency hearing at all (Puria and Allen, 1998; Ruggero and Temchin, 2002; Overstreet and Ruggero, 2002; de La Rochefoucauld et al. 2010).

The behavioural audiogram of the fox appears somewhat more sharply tuned than that of the cat, featuring a narrower region of best sensitivity centred around 4 kHz (Figure 5). In principle, sharper tuning could be the result of a middle ear apparatus of both higher mass and stiffness (Wilson and Bruns, 1983). However, similarities in mass, volume and apparent ossicular stiffness offer no clear reason to suggest that the middle ear apparatus is the underlying cause of this apparent difference in audiograms.

### 4.2 | Inner ear

The red fox inner ear is very similar to that of the cat. The organ of Corti of the red fox contains all typical mammalian structures and cell types. BM length and the total number of hair cells are very similar in the three species. The width of BM at the base is similar in the fox and cat, but it is considerably broader in the dog (Figure 6). The red fox cochlear
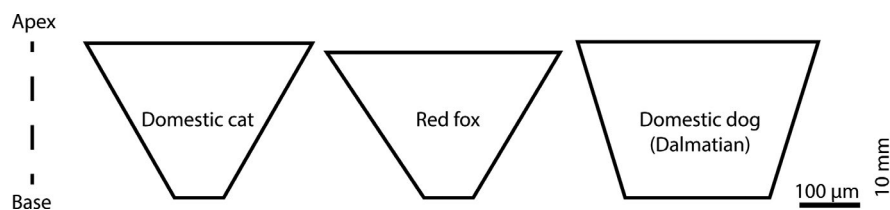


**FIGURE 6** Basal-apical width gradient of the basilar membrane (BM) in the cat, the red fox and the dog. In all species, the width of the BM decreases from apex to the base. Note the similarity between the cat and red fox BM width gradients, and the broad basal BM of the domestic dog. Domestic cat data from Cabezudo (1978); domestic dog (Dalmatian) data from Braniš and Burda (1985)

coiling (3.4 turns) is similar to that of dogs (3–3.5 turns; Gray, 1907; Keen, 1939; Le and Keithley, 2007; Ekdale, 2013) and the domestic cat (3 turns; Gray, 1907; Keen, 1939; Ekdale, 2013). Interestingly, the much bigger tiger and jaguar have only 2.75 turns (Burda et al. 1984); thus, even though BM length has been shown to correlate with body mass (Vater and Kössl, 2011) and the BMs of the tiger and jaguar are considerably longer than that of the cat (Table 2), the coiling of the cochlea appears to be decoupled from this relationship, at least in felids.

Although we did not investigate the vestibular system in detail, it is worth noting that we identified a fusion of the lateral and posterior semicircular canals forming a secondary crus commune. Among extant placental mammals, a secondary crus commune has been described only in the dog (Ekdale, 2013) and certain afrotherian species including aardvark and golden moles (Ekdale, 2013; Mason et al. 2018). It is not found in the cat (Ekdale, 2013). Our finding of a secondary crus commune in the red fox indicates that this unusual feature of unknown functional significance might be common to the Canidae.

### 4.2.1 | Cochlear curvature

The ratio between the curvature of the cochlea at the basal to the apical end was found to be strongly related to low-frequency sensitivity in mammals (Manoussaki et al. 2008). The biggest difficulty in calculating this ratio from our fox scan is that the radius of curvature continues to decline along the length of the cochlear duct as the apex is approached. The apical radius of curvature should be measured along the last quarter-turn of the BM, but the BM cannot be seen in our CT scan. The radius ratio using the last quarter-turn of the cochlear duct was estimated as 10.2, while taking the apical measurement between 45 and 135 degrees from the end of the cochlear duct (based on the assumption that the BM does not extend to the very end) yielded a reduced ratio of 8.6. Both ratios are higher than the value of 6.2 calculated by Manoussaki et al. for the cat. They result in low-frequency hearing limit predictions for the fox of 7 and 19 Hz respectively, both rather lower than the behavioural low-frequency limit of 51 Hz, which is very similar to that of the cat (Figure 5).

### 4.2.2 | Basilar membrane

The dog and cat BM lengths reported in the present study correspond well with data from Braniš and Burda (1985) and Liberman (1982), respectively, studies that used surface specimens just as we did in the present study. Shorter BM lengths have previously been reported for the cat and dog (Table 2), but, in those studies, measurements were made from either serial sections or mid-modiolar sections (Guild, 1921), methods which are prone to underestimate the actual BM length (Greenwood, 1990). The considerably longer BM lengths of the jaguar and the tiger (Burda et al. 1984; surface specimens) fit a positive correlation with body size that has been obvious in datasets reported previously (Echteler et al. 1994). Unfortunately,

no audiograms are available for these large felid species. Comparing a wide range of species, West (1985) demonstrated a positive correlation between the hearing range and the length of the BM. Because BM lengths are similar in all three species included in the present study, no significant differences in hearing range would be expected based on this relationship.

The oscillatory behaviour of the BM determines the tonotopic frequency distribution of hair cells and thus the frequency range represented along the cochlear duct. The BM width and thickness, and the stiffness derived from these parameters have been used for interspecies comparisons and estimates of upper and lower hearing limits (Echteler et al. 1994). With some highly specialized species as exceptions, BM width decreases and BM thickness increases towards the base of the cochlea. The steepness of this gradient, as well as the endpoints, vary from species to species, and are correlated with lifestyle and body size (Vater and Kössl, 2011). High-frequency specialists, such as dolphins and bats, are characterised by a narrow and stiff BM, in particular in the basal region. Low-frequency specialists, such as mysticete whales and mole-rats, are characterised by a wide BM. Based on anatomical data, the red fox would appear to be an auditory generalist, with neither an extremely stiff base, nor an extremely wide apical region, a conclusion which agrees with its behavioral audiogram. Given that cats appear to have better high-frequency sensitivity, we would expect that the cat BM would be stiffer at the basal end, but its anatomical dimensions (thickness, width) are strikingly similar to those of the red fox (Cabezudo, 1978; Echteler et al. 1994). Interestingly, the Dalmatian dog has a much broader BM at the base than the cat and fox (Figure 6, Braniš and Burda, 1985). Fleischer (1973) observed an increased width of the basal BM in dogs of three different breeds (boxer, borzoi, poodle) compared to the wolf, and interpreted this as a consequence of domestication, resulting in reduced high-frequency hearing sensitivity due to a reduced demand for sound localization (see Heffner and Heffner, 2016 for the relationship between high-frequency hearing and sound localization). However, the available audiograms of dogs show comparable high-frequency hearing limits to foxes, raising the question of what a broader BM at the cochlear base in dogs might signify.

### 4.2.3 | Hair cells

The cochlea of the red fox accommodates a similar number of hair cells to those found in the cat and dog (beagle). All three species studied showed the highest average IHC density near the basal end of the cochlear duct (70–90%), a region that might encompass the frequency range of best hearing. In the red fox, this region also showed a thickened stria vascularis, indicative of higher metabolic demands. The minimal and maximal lengths of OHCs, which are related to their frequency responses, are similar in the fox to those reported for the cat (Nadol, 1988; Echteler et al. 1994). We did not detect any significant differences in hair cell densities between the three species we studied. The total numbers of IHCs and OHCs appear to be related

to the length of the BM. Both the BM length and hair cell numbers are almost identical in the fox, cat and dog, while both measures are ~25% higher in the tiger and jaguar (Table 2).

## 4.2.4 | Conclusion

In conclusion, we have presented a detailed anatomical account of the ear of the red fox, which reveals substantial intra-specific variation, partly attributed to age differences. Our anatomical dataset represents the first of its kind for a wild species of similar size to the well-studied domesticated dog and cat.

Foxes, dogs and cats have similar behavioural audiograms, although cats have been found to have better high-frequency hearing and the fox audiogram appears more sharply tuned. If these differences are real, they are not reflected in inner ear structure, which differs relatively little in these species. The similar hearing of cats, dogs and foxes at low frequencies is to be expected on the basis of the similar middle ear cavity volumes and (qualitatively assessed) ossicular stiffnesses. Ossicular mass does not appear to correlate well with high-frequency hearing limits. It is not easy to explain why the fox appears to have a more sharply tuned behavioural audiogram than the dog or cat, and the presence or absence of a bullar bony septum has no obvious effect on the behavioural audiograms.

The models and correlations that we considered in the present study have previously been used to identify broad morpho-functional relationships across mammals in general. We have shown that it is difficult to translate between structure and function among closely-related species of similar size, where differences are more subtle. Species with ostensibly very similar ear structures might still differ in terms of biomechanical properties which are not easily established from anatomical measurements, such as ossicular chain damping or cochlear impedance. Doubtless, hearing is also influenced by other properties of the auditory system, such as molecular adaptations of the hair cells and neuronal components. For those interested in making predictions about hearing from ear morphology, it will be reassuring to note that the three species considered here, which have anatomically similar middle and inner ear structures, do have behavioural audiograms of broadly similar shape. However, we would caution against putting too much emphasis on small differences in peripheral auditory structures when it comes to inferring the hearing attributes of related species.

## CONFLICTS OF INTEREST
None declared.

## DATA AVAILABILITY STATEMENT
A raw dataset related to this publication can be found at: DOI: 10.17632/fn6f98ckd7.1

## ORCID
*Erich Pascal Malkemper* https://orcid.org/0000-0003-1099-0119
*Matthew J. Mason* https://orcid.org/0000-0001-7845-0720
*Hynek Burda* https://orcid.org/0000-0003-2618-818X

## REFERENCES
Ballast, L. (1984) Funktionelle und vergleichende Morphologie der Cochlea von Wildformen und Laborstämmen der Muridae. Unpublished Diss., Frankfurt am Main, Germany: Johann Wolfgang Goethe-Universität.

Begall, S. and Burda, H. (2006) Acoustic communication and burrow acoustics are reflected in the ear morphology of the coruro (*Spalacopus cyanus*, Octodontidae), a social fossorial rodent. *Journal of Morphology*, 267, 382–390.

Bondy, G. (1907) Beiträge zur Vergleichenden Anatomie des Gehörorgans der Säuger (Tympanicum, Membrane Shrapnelli und Chordaverlauf). *Anatomische Hefte*, 35, 293–408.

Braniš, M. and Burda, H. (1985) Inner ear structure in the deaf and normally hearing Dalmatian dog. *Journal of Comparative Pathology*, 95, 295–299.

Burda, H. (1985) Effects of domestication on morphometry of ear structures in Norway rats. *Fortschritte der Zoologie*, 30, 657–659.

Burda, H., Ballast, L. and Bruns, V. (1988) Cochlea in old world mice and rats (Muridae). *Journal of Morphology*, 198, 269–285.

Burda, H., Úlehlová, L. and Braniš, M. (1984) Morphology of the middle and inner ear in two *Panthera* species—*P. tigris* and *P. onca* (Felidae, Carnivora, Mammalia). *Věstník Československé společnosti zoologické*, 48, 9–14.

Cabezudo, L.M. (1978) The ultrastructure of the basilar membrane in the cat. *Acta Oto-laryngologica*, 86, 160–175.

Cole, L.K. (2009) Anatomy and physiology of the canine ear. *Veterinary Dermatology*, 20, 412–421.

Coleman, M.N. and Colbert, M.W. (2010) Correlations between auditory structures and hearing sensitivity in non-human primates. *Journal of Morphology*, 271, 511–532.

Coleman, M.N. and Ross, C.F. (2004) Primate auditory diversity and its influence on hearing performance. *The Anatomical Record A*, 281, 1123–1137.

Dahmann, H. (1929) Zur Physiologie des Hörens; experimentelle Untersuchungen über die Mechanik der Gehörknöchelchenkette, sowie über deren Verhalten auf Ton und Luftdruck. *Z. Hals-Nasen-u Ohrenheilk (Leipzig)*, 24, 462–498.

Dallos, P. (1973) *The Auditory Periphery*. New York, NY: Academic Press.

Davis, H. (1953) Acoustic trauma in the guinea pig. *The Journal of the Acoustical Society of America*, 25, 1180–1189.

de La Rochefoucauld, O., Kachroo, P. and Olson, E.S. (2010) Ossicular motion related to middle ear transmission delay in gerbil. *Hearing Research*, 270, 158–172.

Decraemer, W.F. and Khanna, S.M. (2004) Measurement, visualization and quantitative analysis of complete three-dimensional kinematical

data sets of human and cat middle ear. In: Gyo, K., Wada, H., Hato, N. and Koike, T. (Eds.) _Middle Ear Mechanics in Research and Otology_. Singapore City, Singapore: World Scientific, pp. 3–10.

Defalque, V., Rosenstein, D. and Rosser, J.E. (2005) Measurement of normal middle ear cavity volume in mesaticephalic dogs. _Veterinary Radiology & Ultrasound_, 46, 490–493.

Doran, A. (1878) _Morphology of the mammalian ossicula auditûs_. 2nd series. London: Transactions of the Linnean Society, (Vol. 1, pp. 371-497).

Echteler, S.M., Fay, R.R. and Popper, A.N. (1994) Structure of the mammalian cochlea. In: Fay, R.R. and Popper, A.N. (Eds.) _Comparative Hearing: Mammals_. New York, NY: Springer, pp. 134–171.

Ekdale, E.G. (2013) Comparative anatomy of the bony labyrinth (inner ear) of placental mammals. _PLoS ONE_, 8, e66624.

Evans, H.E. and De Lahunta, A. (2013) _Miller's Anatomy of the Dog_. St. Louis, Missouri: Elsevier Saunders.

Fay, R.R. (1988) _Hearing in Vertebrates: A Psychophysics Databook_. Winnetka, IL: Hill-Fay Associates.

Fleischer, G. (1973) Studien am Skelett des Gehörorgans der Säugetiere, einschließlich des Menschen. _Säugetierkundliche Mitteilungen_, 21, 131–239.

Fleischer, G. (1978) Evolutionary principles of the mammalian middle ear. _Advances in Anatomy, Embryology and Cell Biology_, 55, 1–70.

Fletcher, N.H. (1992) _Acoustic Systems in Biology_. Oxford, UK: Oxford University Press.

Funnell, W.R.J., Decraemer, W.F. and Khanna, S.M. (1987) On the damped frequency response of a finite-element model of the cat eardrum. _The Journal of the Acoustical Society of America_, 81, 1851–1859.

Funnell, W.R.J., Khanna, S.M. and Decraemer, W.F. (1992) On the degree of rigidity of the manubrium in a finite-element model of the cat eardrum. _The Journal of the Acoustical Society of America_, 91, 2082–2090.

Gray, A.A. (1907) _The Labyrinth of Animals. Including Mammals, Birds, Reptiles and Amphibians_. London, UK: J. & A. Churchill.

Greenwood, D.D. (1990) A cochlear frequency-position function for several species—29 years later. _The Journal of the Acoustical Society of America_, 87, 2592–2605.

Guild, S.R. (1921) A graphic reconstruction method for the study of the organ of Corti. _The Anatomical Record_, 22, 140–157.

Guinan, J.J. and Peake, W.T. (1967) Middle-ear characteristics of anesthetized cats. _The Journal of the Acoustical Society of America_, 41, 1237–1261.

Hartová-Nentvichová, M., Anděra, M. and Hart, V. (2010) Cranial ontogenetic variability, sex ratio and age structure of the red fox. _Central European Journal of Biology_, 5, 894–907.

Heffner, H.E. (1983) Hearing in large and small dogs: Absolute thresholds and size of the tympanic membrane. _Behavioral Neuroscience_, 97, 310–318.

Heffner, H.E. and Heffner, R.S. (2016) The evolution of mammalian sound localization. _Acoustics Today_, 12, 20–27.

Hemilä, S., Nummela, S. and Reuter, T. (1995) What middle ear parameters tell about impedance matching and high frequency hearing. _Hearing Research_, 85, 31–44.

Holz, K. (1931) Vergleichende anatomische und topographische Studien über das Mittelohr der Säugetiere. _Zeitschrift für Anatomie und Entwicklungsgeschichte_, 94, 757–791.

Huang, G., Rosowski, J. and Peake, W. (2000) Relating middle-ear acoustic performance to body size in the cat family: measurements and models. _Journal of Comparative Physiology A_, 186, 447–465.

Huang, G., Rosowski, J., Ravicz, M. and Peake, W. (2002) Mammalian ear specializations in arid habitats: structural and functional evidence from sand cat (_Felis margarita_). _Journal of Comparative Physiology A_, 188, 663–681.

Hunt, R.M. (1974) The auditory bulla in Carnivora: an anatomical basis for reappraisal of carnivore evolution. _Journal of Morphology_, 143, 21–75.

Hunt, R.M. and Korth, W.W. (1980) The auditory region of Dermoptera: morphology and function relative to other living mammals. _Journal of Morphology_, 164, 167–211.

Igarashi, M., Alford, B., Cohn, A., Saito, R. and Watanabe, T. (1972) Inner ear anomalies in dogs. _The Annals of Otology, Rhinology, and Laryngology_, 81, 249–255.

Keen, J.A. (1939) A note on the comparative size of the cochlear canal in mammals. _Journal of Anatomy_, 73, 592.

Keen, J.A. (1940) A note on the length of the basilar membrane in man and in various mammals. _Journal of Anatomy_, 74, 524.

Keen, J.A. and Grobbelaar, C.S. (1941) The comparative anatomy of the tympanic bulla and auditory ossicles, with a note suggesting their function. _Transactions of the Royal Society of South Africa_, 28, 307–329.

Ketten, D.R. (1997) Structure and function in whale ears. _Bioacoustics_, 8, 103–135.

Kirikae, I. (1960) _The structure and function of the middle ear_. Tokyo, Japan: University of Tokyo Press.

Lavender, D., Taraskin, S.N. and Mason, M.J. (2011) Mass distribution and rotational inertia of "microtype" and "freely mobile" middle ear ossicles in rodents. _Hearing Research_, 282, 97–107.

Le, T. and Keithley, E.M. (2007) Effects of antioxidants on the aging inner ear. _Hearing Research_, 226, 194–202.

Liberman, M.C. (1982) The cochlear frequency map for the cat: labeling auditory-nerve fibers of known characteristic frequency. _The Journal of the Acoustical Society of America_, 72, 1441–1449.

Liberman, M.C. and Beil, D.G. (1979) Hair cell condition and auditory nerve response in normal and noise-damaged cochleas. _Acta Otolaryngologica_, 88, 161–176.

Lynch, T.J., Nedzelnitsky, V. and Peake, W.T. (1982) Input impedance of the cochlea in cat. _The Journal of the Acoustical Society of America_, 72, 108–130.

Mair, I. (1976) Hereditary deafness in the Dalmatian dog. _European Archives of Oto-Rhino-Laryngology_, 212, 1–14.

Malkemper, E.P. and Peichl, L. (2018) Retinal photoreceptor and ganglion cell types and topographies in the red fox (_Vulpes vulpes_) and Arctic fox (_Vulpes lagopus_). _Journal of Comparative Neurology_, 2018, 1–21.

Malkemper, E.P., Topinka, V. and Burda, H. (2015) A behavioral audiogram of the red fox (_Vulpes vulpes_). _Hearing Research_, 320, 30–37.

Manoussaki, D., Chadwick, R.S., Ketten, D.R., Arruda, J., Dimitriadis, E.K. and O'Malley, J.T. (2008) The influence of cochlear shape on low-frequency hearing. _Proceedings of the National Academy of Sciences of the United States of America_, 105, 6162–6166.

Mason, M. (1999) _The functional anatomy of the middle ear of mammals, with an emphasis on fossorial forms_. Unpublished Ph. D. Diss., Cambridge, UK: Univ. of Cambridge.

Mason, M.J. (2003) Bone conduction and seismic sensitivity in golden moles (Chrysochloridae). _Journal of Zoology, London_, 260, 405–413.

Mason, M.J. (2004) Functional morphology of the middle ear in _Chlorotalpa_ golden moles (Mammalia, Chrysochloridae): predictions from three models. _Journal of Morphology_, 261, 162–174.

Mason, M.J. (2006) Evolution of the middle ear apparatus in talpid moles. _Journal of Morphology_, 267, 678–695.

Mason, M.J. (2013) Of mice, moles and guinea pigs: Functional morphology of the middle ear in living mammals. _Hearing Research_, 301, 4–18.

Mason, M.J. (2016a) Structure and function of the mammalian middle ear. I: Large middle ears in small desert mammals. _Journal of Anatomy_, 228, 284–299.

Mason, M.J. (2016b) Structure and function of the mammalian middle ear. II: Inferring function from structure. _Journal of Anatomy_, 228, 300–312.

Mason, M.J., Bennett, N.C. and Pickford, M. (2018) The middle and inner ears of the Palaeogene golden mole _Namachloris_: a comparison with extant species. _Journal of Morphology_, 279, 375–395.

Mason, M.J., Cornwall, H.L. and Smith, E.S.J. (2016) Ear structures of the naked mole-rat, *Heterocephalus glaber*, and its relatives (Rodentia: Bathyergidae). *PLoS ONE*, 11, e0167079.

Montague, M.J., Li, G., Gandolfi, B., et al. (2014) Comparative analysis of the domestic cat genome reveals genetic signatures underlying feline biology and domestication. *Proceedings of the National Academy of Sciences of the United States of America*, 111, 17230–17235.

Mooney, M.P., Kraus, E.M., Bardach, J. and Snodgass, J.I. (1982) Skull preparation using the enzyme-active detergent technique. *The Anatomical Record*, 202, 125–129.

Nadol, J.B. Jr (1988) Comparative anatomy of the cochlea and auditory nerve in mammals. *Hearing Research*, 34, 253–266.

Nedzelnitsky, V. (1980) Sound pressures in the basal turn of the cat cochlea. *The Journal of the Acoustical Society of America*, 68, 1676–1689.

Nummela, S. (1995) Scaling of the mammalian middle ear. *Hearing Research*, 85, 18–30.

Overstreet, E.H. and Ruggero, M.A. (2002) Development of wide-band middle ear transmission in the Mongolian gerbil. *The Journal of the Acoustical Society of America*, 111, 261–270.

Peake, W.T., Rosowski, J.J. and Lynch Iii, T.J. (1992) Middle-ear transmission: Acoustic versus ossicular coupling in cat and human. *Hearing Research*, 57, 245–268.

Puria, S. and Allen, J.B. (1998) Measurements and model of the cat middle ear: evidence of tympanic membrane acoustic delay. *The Journal of the Acoustical Society of America*, 104, 3463–3481.

Ravicz, M.E., Rosowski, J.J. and Voigt, H.F. (1992) Sound-power collection by the auditory periphery of the Mongolian gerbil *Meriones unguiculatus*. I: Middle-ear input impedance. *The Journal of the Acoustical Society of America*, 92, 157–177.

Retzius, G. (1884) *Das Gehörorgan der Wirbelthiere: morphologisch-histologische Studien. 2, Das Gehörorgan der Reptilien, der Vögel und der Säugethiere*. Stockholm, Sweden: Gedruckt in der Centraldruckerei in Commission bei Samson & Wallin.

Rosowski, J. (1992) Hearing in transitional mammals: predictions from the middle-ear anatomy and hearing capabilities of extant mammals. In: Webster, D.B., Popper, A.N. and Fay, R.R. (Eds.) *The Evolutionary Biology of Hearing*. New York, NY: Springer, pp. 615–631.

Rosowski, J.J. and Graybeal, A. (1991) What did *Morganucodon* hear? *Zoological Journal of the Linnean Society*, 101, 131–168.

Rosowski, J.J., Ravicz, M.E. and Songer, J.E. (2006) Structures that contribute to middle-ear admittance in chinchilla. *Journal of Comparative Physiology A*, 192, 1287–1311.

Ruggero, M.A. and Temchin, A.N. (2002) The roles of the external, middle, and inner ears, in determining the bandwidth of hearing. *Proceedings of the National Academy of Sciences of the United States of America*, 99, 13206–13210.

Salih, W.H.M., Buytaert, J.A.N., Aerts, J.R.M., Vanderniepen, P., Dierick, M. and Dirckx, J.J.J. (2012) Open access high-resolution 3D morphology models of cat, gerbil, rabbit, rat and human ossicular chains. *Hearing Research*, 284, 1–5.

Sato, M., Leake, P.A. and Hradek, G.T. (1999) Postnatal development of the organ of Corti in cats: a light microscopic morphometric study. *Hearing Research*, 127, 1–13.

Schleich, C.E. and Busch, C. (2004) Functional morphology of the middle ear of *Ctenomys talarum* (Rodentia: Octodontidae). *Journal of Mammalogy*, 85, 290–295.

Schuknecht, H.F. (1953) Techniques for study of cochlear function and pathology in experimental animals. *AMA Archives of Otolaryngology*, 58, 377–397.

Schuknecht, H.F., Icarashi, M. and Gacek, R.R. (1965) The pathological types of cochleo-saccular degeneration. *Acta Oto-laryngologica*, 59, 154–170.

Solntseva, G. (2010) Morphology of the inner ear of mammals in ontogeny. *Russian Journal of Developmental Biology*, 41, 94–110.

Solntseva, G. (2013) Adaptive features of the middle ear of mammal in ontogeny. *Acta Zoologica Bulgarica*, 65, 101–116.

Spoendlin, H. (1969) Innervation patterns in the organ of Corti of the cat. *Acta Oto-Laryngologica*, 67, 239–254.

Ulehlova, L., Burda, H. and Voldrich, L. (1984) Involution of the auditory neuro-epithelium in a tiger (*Panthera tigris*) and a jaguar (*Panthera onca*). *Journal of Comparative Pathology*, 94, 153–157.

van Kampen, P.N. (1905) Die Tympanalgegend des Säugetierschädels. *Gegenbaurs Morphologisches Jahrbuch*, 34, 321–327.

Vater, M. and Kössl, M. (2011) Comparative aspects of cochlear functional organization in mammals. *Hearing Research*, 273, 89–99.

von Békésy, G. (1960) *Experiments in Hearing*. New York, NY: McGraw-Hill.

Webster, D.B. and Webster, M. (1975) Auditory systems of Heteromyidae: functional morphology and evolution of the middle ear. *Journal of Morphology*, 146, 343–376.

West, C.D. (1985) The relationship of the spiral turns of the cochlea and the length of the basilar membrane to the range of audible frequencies in ground dwelling mammals. *The Journal of the Acoustical Society of America*, 77, 1091–1101.

West, C.D. and Harrison, J.M. (1973) Transneuronal cell atrophy in the congenitally deaf white cat. *Journal of Comparative Neurology*, 151, 377–398.

Wible, J.R. and Spaulding, M. (2012) A reexamination of the Carnivora malleus (Mammalia, Placentalia). *PLoS ONE*, 7, e50485.

Wilson, J. and Bruns, V. (1983) Middle-ear mechanics in the CF-bat *Rhinolophus ferrumequinum*. *Hearing Research*, 10, 1–13.

Zwislocki, J. (1965) *Analysis of Some Auditory Characteristics*. Handbook of Mathematical Psychology. New York, NY: Wiley.

## SUPPORTING INFORMATION

Additional supporting information may be found online in the Supporting Information section.